iScience

CellPress
OPEN ACCESS

Article

Impaired tryptophan metabolism by type 2 inflammation in epithelium worsening asthma

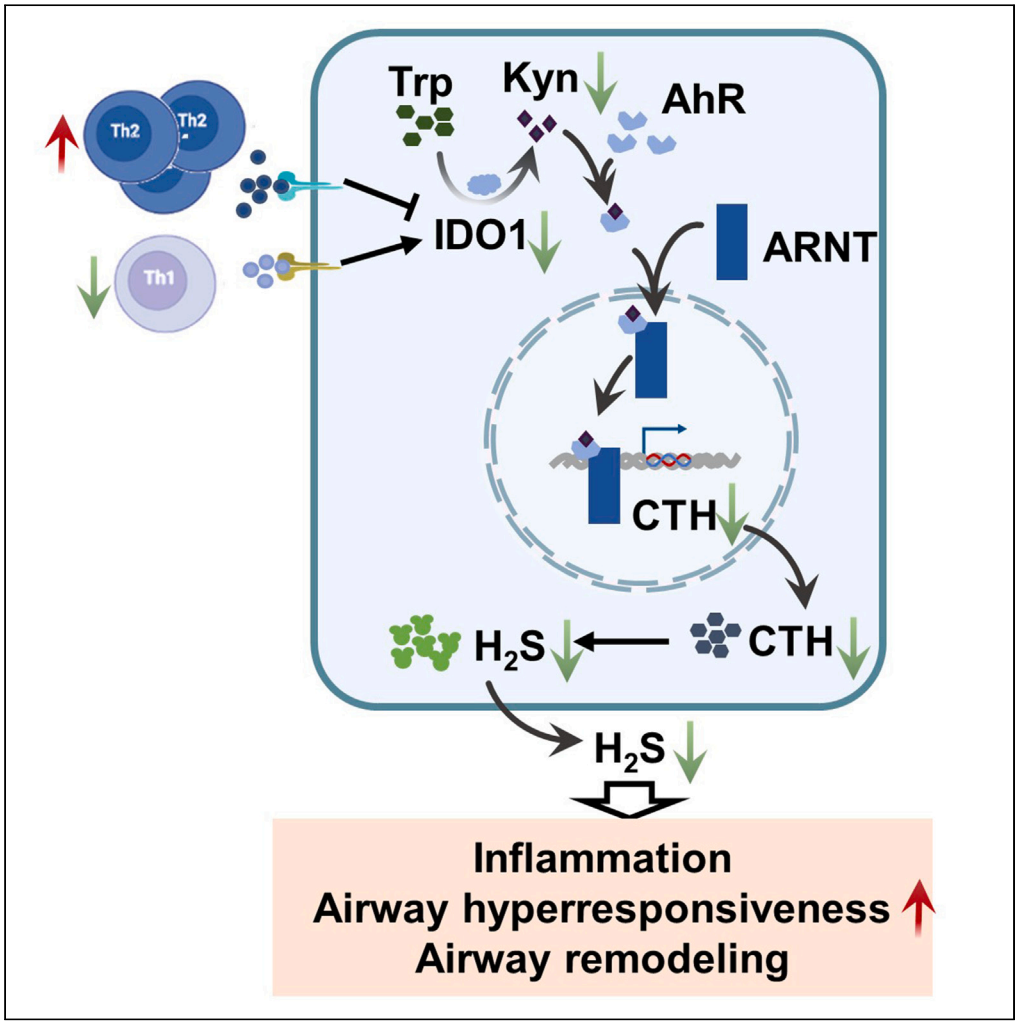

Yushan Miao (缪瑜姗), Caiming Zhong (仲彩铭), Shujun Bao (包淑钧), ..., Chong Bai (白冲), Wei Chen (谌卫), Hao Tang (唐昊)

bc7878@sohu.com (C.B.)
wujiang02@163.com (W.C.)
tanghao_0921@126.com (H.T.)

Highlights

In allergic asthma, tryptophan metabolism was hampered by T2 inflammation

CTH can be regulated by tryptophan metabolism through AhR

IDO1-Kyn-CTH pathway could be a potential target for treatment for allergic asthma

Miao et al., iScience 27, 109923
June 21, 2024
https://doi.org/10.1016/j.isci.2024.109923

iScience

CellPress
OPEN ACCESS

Article

Impaired tryptophan metabolism by type 2 inflammation in epithelium worsening asthma

Yushan Miao (缪瑜姗),[1,2,5] Caiming Zhong (仲彩铭),[1,2,5] Shujun Bao (包淑钧),[1,5] Kunchen Wei (韦坤辰),[1] Wei Wang (王伟),[1] Na Li (李娜),[3] Chong Bai (白冲),[2,*] Wei Chen (谌卫),[4,*] and Hao Tang (唐昊)[1,6,*]

SUMMARY

Previous researches indicate that tryptophan metabolism is critical to allergic inflammation and that indoleamine 2,3-dioxygenase 1 (IDO1), as a key enzyme, is known for its immunosuppressive properties. Therefore, we are aimed to explore whether tryptophan metabolism, especially IDO1, influences allergic asthma and clarify specific mechanism. With the analysis of clinical data, exploration in cell experiments, and verifying in HDM-induced asthma mice models, we finally found that in allergic asthma, low level of T1 cytokines along with high level of T2 cytokines inhibited the expression of IDO1 in airway epithelium, hampering the kynurenine pathway in tryptophan metabolism and decreasing the level of intracellular kynurenine (Kyn). As an endogenous ligand of aryl hydrocarbon receptor, Kyn regulated the expression of cystathionine-γ-lyase (CTH). Notably, in asthma models, enhancing either IDO1 or H_2S relieved asthma, while inhibiting the activity of CTH exacerbated it. IDO1-Kyn-CTH pathway could be a potential target for treatment for allergic asthma.

INTRODUCTION

Asthma is characterized as airway chronic inflammation and immune dysfunction, which results in hyperresponsive airways and airway remodeling. Patients with asthma accounts for 4.2% of the total population,[1] and the population has been rising due to industrialization. Different subtypes of asthma are heterogeneous in clinic and mechanism.[2] Allergic asthma is the most common type of asthma, characterized by a Th2-driven process, high levels of IgE, eosinophils, and type 2 (T2) cytokines, including interleukin (IL)-4, IL-5, and IL-13.[3] However, the underlying mechanism of the disease remains unknown, so current treatments tend to relieve symptoms only not to cure or prevent it.

Recent research has shown that small molecular metabolites, of which tryptophan metabolism is typical, involve in immunity regulation. Only a small portion of the absorbed tryptophan is employed in the synthetic metabolism process, and the majority of tryptophan is metabolized through the kynurenine pathway (KP) into kynurenine, which plays a critical role in the regulation of inflammation, immune responses, neurological functions, and intestinal microenvironment.[4,5] Clinical studies have confirmed that in asthma tryptophan metabolism is impaired.[6] In conclusion, tryptophan metabolism is closely associated with allergic asthma, and the purpose of this article is to clarify the specific roles and mechanism in this process and to provide clues for clinical trials.

The key enzymes of the KP include tryptophan-2,3-dioxygenase (TDO) and indoleamine-2,3-dioxygenase (IDO), which vary widely among different tissues and organs. Additionally, IDO1 is highly expressed in the respiratory system and predominantly localized in parenchymal cells not immune cells.[5] However, most studies only focused on highly tryptophan-depended immune cells such as T cells, dendritic cells, and macrophages.[7] Recent study has shown that in COVID-19 patients, IDO enzymes are differentially expressed in the pulmonary blood vessels.[8] Therefore, we are aimed to explore the role and specific mechanism of IDO1 in epithelium, which is the main cell type in lung.

Aryl hydrocarbon receptor (AhR), as a ligand-activated transcription factor, is involved in the pathological development of several respiratory diseases and plays a key role in immunomodulation, carcinogenesis, and inflammatory responses. AhR was initially found to bind to the aromatic compound 2, 3, 7, 8-tetrachlorodibenzo-P-dioxin, then translocate from the cytosol to the nucleus and dimerize with the AhR nuclear transporter, bind to aromatic hydrocarbon-responsive elements (AhRE, also called XREs or DREs) in the 5′ flanking region of genes, and finally activate the transcription of target genes, such as *CYP1A1*, *CYPIB1*, which have implications as key factors in the respiratory response to environmental toxicants.[9] Kyn, as one of exogenous ligands, can work through AhR, influence the expression of target genes, and have the potential to play a key role in allergic asthma.[10]

[1]Department of Respiratory and Critical Care Medicine, Shanghai Changzheng Hospital, Naval Medical University, Shanghai 200003, China
[2]Department of Respiratory and Critical Care Medicine, Shanghai Changhai Hospital, Naval Medical University, Shanghai 200433, China
[3]School of Medicine, Shanghai University, Shanghai 200444, China
[4]Department of Nephrology, Shanghai Changhai Hospital, Naval Medical University, Shanghai 200433, China
[5]These authors contributed equally
[6]Lead contact
*Correspondence: bc7878@sohu.com (C.B.), wujiang02@163.com (W.C.), tanghao_0921@126.com (H.T.)
https://doi.org/10.1016/j.isci.2024.109923

Further, endogenous hydrogen sulfide, as the third gas transmitter molecule, participates in respiratory diseases, similarly to nitric oxide.[11] Cystathionine-γ-lyase (CTH) is one of the key enzymes for endogenous hydrogen sulfide (H_2S) production. Hydrogen sulfide tends to be beneficial in lung diseases. Disorders in endogenous hydrogen sulfide synthesis and level are associated with accelerated lung aging and the development of asthma, chronic obstructive pulmonary disease, and fibrosis.[12–14]

Therefore, we are intended to explore the level of the tryptophan metabolism and its key enzyme IDO1 in allergic asthma and to clarify the specific mechanism of this process. Additionally, we are aimed to illustrate the effect and mechanism of tryptophan metabolism abnormalities (especially IDO1) on allergic asthma and to make it clear whether IDO1-regulated tryptophan metabolism plays a role in airway remodeling in allergic asthma by affecting the synthesis of endogenous hydrogen sulfide. This study is helpful to gain insight into allergic asthma and can provide clues for the new therapy.

RESULTS

Downregulation of tryptophan metabolism in asthma

We collected blood samples from 10 health control and 17 patients with allergic asthma (Table S1). Analysis on serum cytokines showed the upregulated IL-4 and IL-13 and the downregulated IFN-γ, which confirmed the T2 inflammation (Figures 1A–1C and S1A). We further calculated kynurenine/tryptophan (Kyn/Trp), indicating the level of tryptophan metabolism, and found that tryptophan metabolism was hampered compared to healthy individuals (Figure 1B). Previous studies have shown that cytokines can influence tryptophan metabolism by regulating key enzymes. For example, IFN-γ is a strong activator of IDO,[15] and IL-4I1 is activated by IL-4 in immune cells.[16] Out of this consideration, we found that T1/2 cytokines levels in serum showed a good correlation with Kyn/Trp (Figures 1D–1F).

Furthermore, we collected nontumor lung tissues from surgery cancer patients with or without the medical history of asthma (Table S2). Compared to the control, lung from asthma patients had exacerbated bronchiolar epithelium hyperplasia, goblet cell metaplasia, deposition of subepithelial collagen, thickening of basement membrane and smooth muscle layer, and inflammatory cell infiltration (Figure S1B). Notably, the expression of IDO1, one of the key enzymes of tryptophan metabolism, was decreased in airway epithelium of asthma patients (Figures 1H and S1B).

We also induced allergic asthma with house dust mite (HDM) in mice (Figure S2A). In this model, inflammatory cell infiltration, airway epithelial goblet cell proliferation, increased mucus secretion, and subepithelial fibrosis were apparent (Figures S2B and S2C). Meanwhile, both in serum and in lung, T2 cytokines increased significantly, while T1 cytokines had no significant difference, indicating T2 inflammation (Figures S2D and S2E). Consistently, IDO1 expression in airway epithelium was decreased (Figures 1D–1M).

Aforementioned results indicated that tryptophan metabolism may participate in the process of asthma and that the level of tryptophan metabolism is associated with that of T1/2 cytokines.

T1/2 cytokines regulated tryptophan metabolism to kynurenine in airway epithelium

Based on the findings from clinical data, we hypothesized that T1/2 cytokines can regulate tryptophan metabolism. To verify this hypothesis, we stimulated airway epithelial cells (BEAS-2B) with T1 cytokines (IFN-γ and TGF-β) and T2 cytokines (IL-4, IL-5, and IL-13) and detected four key enzymes of metabolism (IDO1, IDO2, TDO2, and IL-4I1).[5,17] Out of the consideration that the concentration of Trp in medium is possible to influence the results, cells were washed with PBS and then incubated in Ham's F-10 (Gibco), which is Trp-deficient with only 3 μM Trp, and extra 500 μM Trp was added (Figures S3A and S3B). It was found that IDO1 and TDO2 (key enzymes of KP), especially IDO1, was upregulated by IFN-γ (Figure 2A), indicating that KP is the potential pathway regulated by T1/2 cytokines.

Furthermore, a total of 12 types of tryptophan metabolites were detected in airway epithelial cells with or without IFN-γ stimulation (Table S3). Results showed that six metabolites-including tryptophan (Trp), Kyn, N-formyl-kynurenine (NFK), cinnavalininate (CA), 5-hydroxytryptamine (5-HT), and indole-3-carboxaldehyde (I3A)-were significantly different between the two groups (Figures 2B and S3F; Table S4). According to tryptophan metabolism pathways, four out of the previous six metabolites belong to KP, which demonstrates that KP is the primary pathway in this process (Figure S3C). Notably, although the concentration of Trp was increased greatly, the concentration of Kyn elevated mildly with the absence of IFN-γ (Figure S3B). However, the presence of IFN-γ, even if the physiological concentration of IFN-γ, improved the concentration of Kyn and increased Kyn/Trp ratio greatly (Figures 2C–2E). Additionally, to explore whether T2 cytokines participated the regulation of KP, we stimulated cells with IL-4, IL-5, and IL-13. Apparently, T2 cytokines hampered KP and the concentration of Kyn, which are maintained by IFN-γ (Figures 2F–2H). In summary, we investigated the metabolic effect of T1 and T2 cytokines on tryptophan metabolism in airway epithelium and found that KP was the main pathway in this process. Additionally, Kyn, as the key metabolite, was the potential molecule that can exert profound effects on allergic asthma.

IDO1 is the key enzyme regulated by T1/2 cytokines in airway epithelial cells

Key enzymes of KP include IDO1, IDO2, and TDO2, and we found that both IDO1 and TDO2 can be regulated by IFN-γ (Figure 2A). To further illustrate, which key enzyme plays the critical role in this process, we stimulated BEAS-2B with different IDO1 and/or TDO2 inhibitors, and it suggested that IDO1, not TDO2 (another key enzyme in KP), is attributed to the change of KP (Figures S3C–S3E).

Furthermore, IDO1 showed a time- and concentration-dependent enhanced expression in response to IFN-γ stimulation (Figures 3A–3D). Notably, physiological serum concentration (peak level)[18] of IFN-γ was competent to induce IDO1 expression (Figures 3A and 3B). With a peak level of IFN-γ, adding T2 cytokines reduced the transcription and expression level of IDO1 (Figures 3E and 3F). These results showed

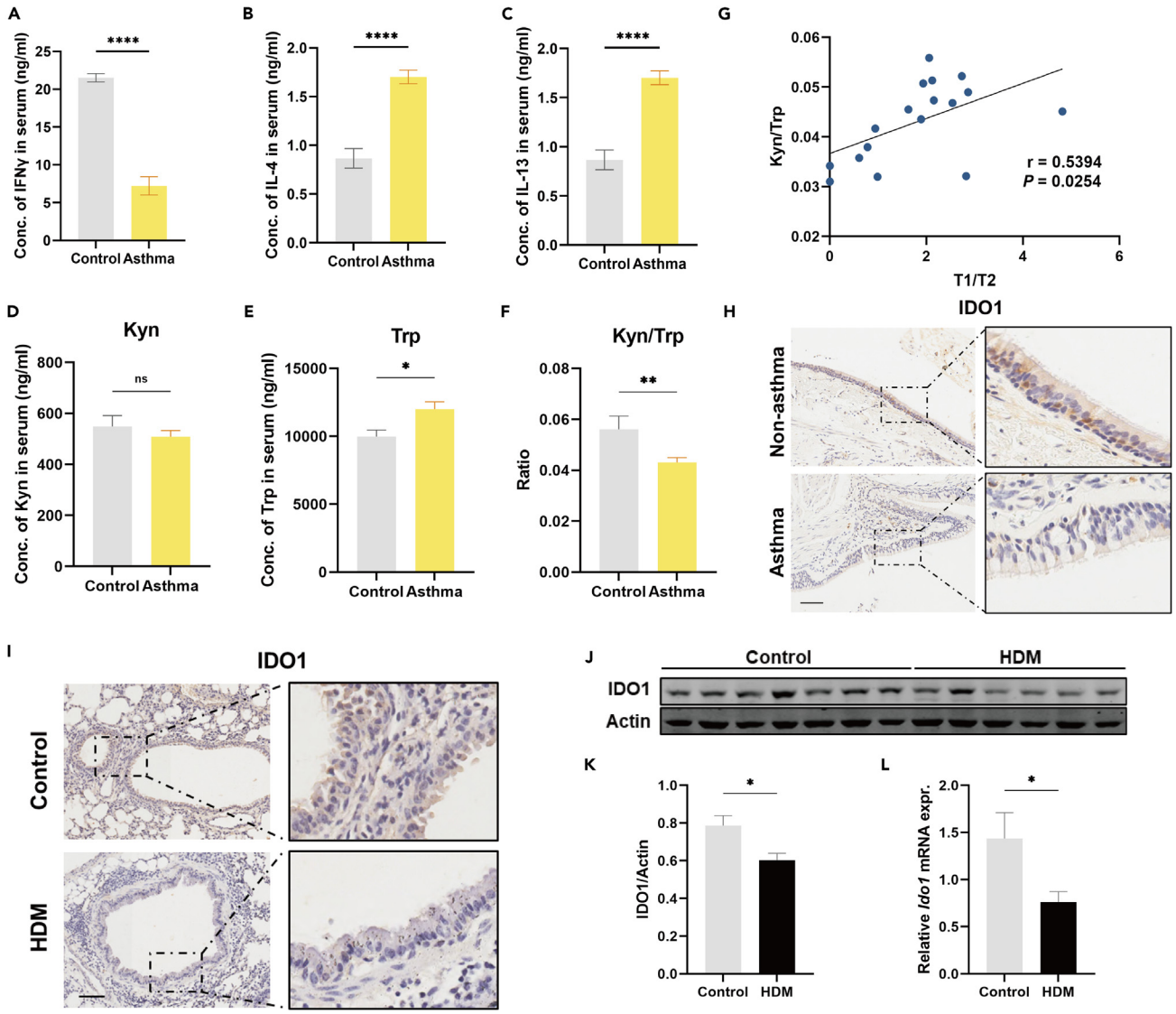

Figure 1. Downregulation of tryptophan metabolism in asthma

(A–C) The levels of cytokines IFN-γ (A), IL-4 (B), and IL-13 (C) in the serum between control and asthma group. Data are represented as mean ± SEM. See also Figure S1A.

(D and E) Serum levels of tryptophan (D) and kynurenine (E) in 10 health and 17 asthma participants were detected by mass spectrometry.

(F) The ratio of Kyn to Trp is presented. Data are represented as mean ± SEM.

(G) Correlation between Kyn/Trp and T1/T2 (IFN-γ/IL4+IL13) is shown.

(H) The representative detail of IDO1 IHC staining images in asthma and matched non-asthma lung tissue. Scale bar, 100 μm. See also Figure S1B.

(I) The expression IDO1 in airway epithelium in mice models was detected by IHC. Scale bar, 100 μm.

(J and K) Western blots (J) and semi-quantitative analysis (K) showed IDO1 levels.

(L) The mRNA level of IDO1 in lung was detected by RT-PCR. One of three repeated experiments with similar results is presented. The animal experiments included 6–7 BALB/c mice in each group. *$p < 0.05$, **$p < 0.01$, ns, not significant. See also Figures S1 and S2 and Tables S1 and S2.

that T1 cytokines can upregulated the expression of IDO1, which can maintain the KP in physical, and that T2 cytokines hampered the expression of IDO1.

Additionally, the knockdown of IDO1 can hamper the upregulated expression of IDO1 by IFN-γ (Figures 3G and S4A), which indicated that the level of mRNA is the key factor influenced by IDO1. JAK is the main downstream of IFN-γ, and we found that Ruxolitinib, a JAK1/2 inhibitor, inhibited the expression of IDO1 induced by IFN-γ through the JAK1/2-STAT3 pathway (Figures 3H, 3I, and S4D). The knockdown of JAK1 also can decrease IDO1 (Figures S4B and S4C). Meanwhile, T2 cytokines inhibited IDO1 expression by regulating JAK2 phosphorylation (Figure 3I). The results previously suggested that JAK1/2-STAT3 pathway is critical in this process.

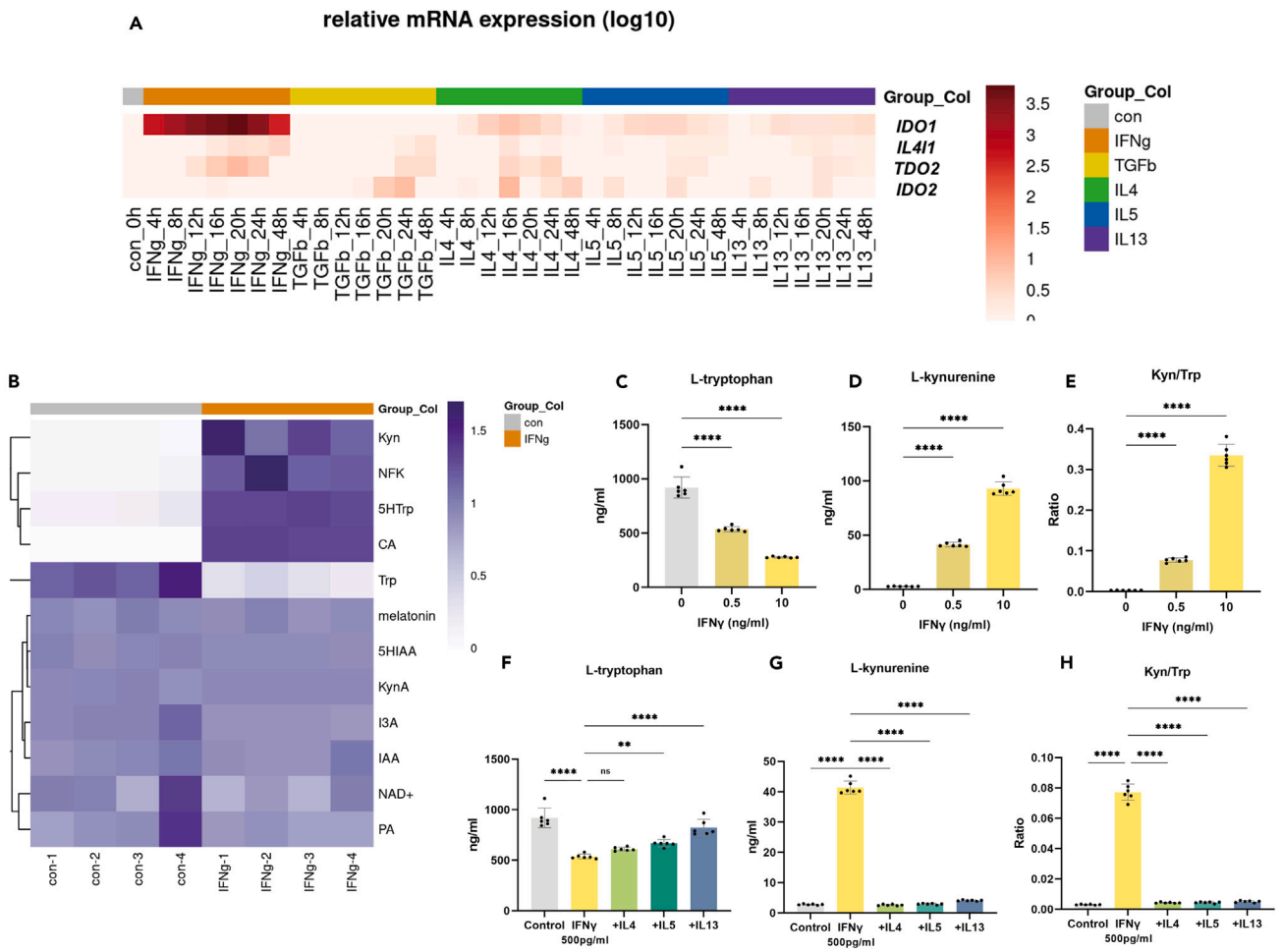

Figure 2. T1/2 cytokines regulated tryptophan metabolism to kynurenine in airway epithelium

(A) The heatmap of relative mRNA levels (log10) of key enzymes (IDO1, IDO2, TDO2, and IL-4I1) in BEAS-2B cells treated with different cytokines (IFN-γ, TGF-β, IL-4, IL-5, and IL-13; all cytokines at 10 ng/mL) at different time points (4, 8, 12, 20, 24, 48 h) is presented.

(B) Heatmap of metabolites related to tryptophan metabolism detected in BEAS-2B with or without 10 ng/mL IFN-γ for 24 h is shown. $n = 4$. See also Figure S2C.

(C and D) The concentration of Trp (C) and Kyn (D) were detected after stimulation with different concentrations of IFN-γ. Data are represented as mean ± SEM.

(E) The ratio of Kyn to Trp after stimulation with different concentrations of IFN-γ is presented. Data are represented as mean ± SEM.

(F and G) The concentration of Trp (C) and Kyn (D) were detected after stimulation with T2 cytokines (IL-4, IL-5, and IL13) at the presence of IFN-γ. Data are represented as mean ± SEM.

(H) The ratio of Kyn to Trp was calculated after treatment with T2 cytokines at the presence of IFN-γ. Data are represented as mean ± SEM. $^{**}p < 0.05$, $^{****}p < 0.01$, ns, not significant. See also Figure S2 and Tables S3 and S4.

Kyn induces AhR translocation to regulate the transcription of the CTH gene

Next, we intended to explore the specific role and mechanism of Kyn, which was the main metabolite we found in this process (Figure S3F). Previous researches have reported that Kyn is one of exogenous ligands of AhR.[10] Therefore, we demonstrated that Kyn induced AhR translocation to the nucleus in airway epithelial cells and regulated its classical gene expression, such as *CYP1B1* (Figures S5A–S5C). Further, by CUT&Tag, we detected genes that can be regulated by AhR and confirmed that 332 genes were upregulated by Kyn and 163 genes were downregulated, most of which were related to cell metabolism, including various toxic substance metabolism and energy metabolism (Figure S6A), in accordance with the classical AhR regulation mode. We sorted out 31 significantly upregulated genes, which may have specific physiological significance (Figure S6B). Among them, *CYP1A1* and *CYP1B1* were classic AhR target genes, and *IL24*, *MUC5AC*, *CTH*, and *IL17REL*, were related to asthma.

Finally, we focused on *CTH* gene that encodes cystathionine-γ-lyase, one of endogenous hydrogen sulfide synthetases, expressed primarily in the airway. We confirm that the specific binding site of the AHRE response element is at position 34–38 in the first exon of *CTH* gene (Figure S6C). Then we designed primers that crossed this site to further verify this result by ChIP-RT-PCR (Figure 4A).

The overexpression of IDO1 in BEAS-2B also induced the expression of CTH (Figure 4B). Additionally, knocking down the expression of IDO1 influenced the mRNA level of CTH (Figure 4C). Meanwhile, IFN-γ and Kyn increased the expression of CTH along with IDO1, while T2

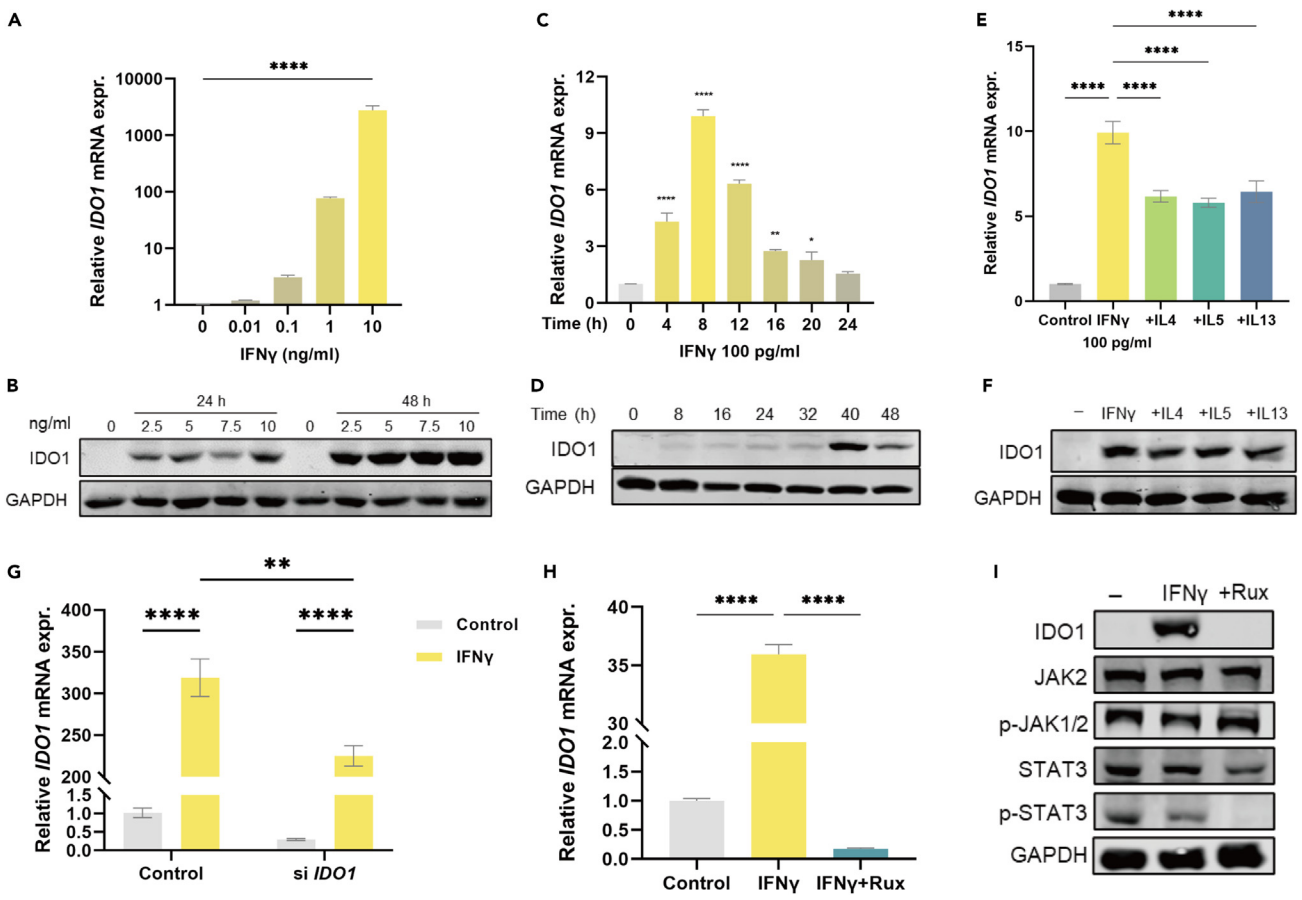

Figure 3. IDO1 is the key enzyme regulated by T1/2 cytokines in airway epithelial cells

(A) Relative mRNA level of IDO1 in BEAS-2B cells was measured after 12 h - treatment with IFN-γ at 0, 0.01, 0.1, 1 ng/mL, 10 ng/mL by RT-PCR. Data are represented as mean ± SEM.

(B) IDO1 protein level was detected by western blot in BEAS-2B cells 24 and 48 h after treatment with IFN-γ at 0, 2.5, 5, 7.5, 10 ng/mL.

(C and D) The expression of IDO1 at transcription (C) and expression (D) levels at different time points after IFN-γ stimulation at 100 pg/mL in BEAS-2B cells. Data are represented as mean ± SEM.

(E and F) IDO1 mRNA levels after 12 h (E) and protein level after 24 h (F) in BEAS-2B after stimulation of 10 ng/mL IL-4, IL-5, and IL-13 at the presence of 100 pg/mL IFN-γ. Data are represented as mean ± SEM.

(G) IDO1 mRNA levels in BEAS-2B (pretreated with si IDO1 or control) after stimulation of 10 ng/mL IFN-γ. Data are represented as mean ± SEM.

(H) IDO1 expression was detected by RT-PCR after 12 h—treatment with or without Ruxolitinib (5 μM) in the presence of IFN-γ (10 ng/mL). Data are represented as mean ± SEM.

(I) Western blots showed IDO1 and JAK-STAT pathway proteins level in BEAS-2B cells after 24 h stimulation of IFN-γ (10 ng/mL) with or without Ruxolitinib (5 μM). Rux, Ruxolitinib, JAK1/2 inhibitor. Data in A, C, E, and G are means ± SEM. One-way analysis of variance (ANOVA) was performed in A, C, E, and G. One of three experiments with similar results is presented. *$p < 0.05$, **$p < 0.01$, ****$p < 0.0001$. See also Figure S4.

cytokines inhibited that (Figures 4D–4G and S5D). It was also found that CTH expression was inhibited after the inhibition of IDO1 and AhR translocation (Figure 4I). The results suggested that IDO1-Kyn-AhR stimulated the expression of CTH by affecting AhR translocation.

We also examined the expression of CTH in mice model and found that the expression trend of CTH was the same as that of IDO1 (Figures 1D–1G, 4H, and S5E–S5G), which suggested the IDO1-Kyn-CTH regulation pathway *in vivo*.

IDO1 overexpression relieved HDM-induced allergic asthma

To investigate whether IDO1 has the potential to protect against asthma, we infected lung tissues of mice were with pneumophilic adeno-associated virus (AAV) carrying the *Ido1* gene to upregulate the expression of IDO1 in lungs (Figure S7A). Neither AAV infection nor the expression of additional IDO1 affected the pathological state of lungs in mice. In allergic asthma, compared with mice infected by AAV-control, mice infected by AAV-*Ido1* had less inflammatory infiltration, airway epithelial goblet cell proliferation, and subepithelial fibrosis (Figures 5A–5D).

Additionally, the expression of CTH was upregulated in AAV-*Ido1* infected both control and asthma mice, and the depletion of CTH was compensated in AAV-*Ido1* infected mice (Figures 5E and 5F), which confirmed that the expressions of IDO1 and CTH are impaired in allergic

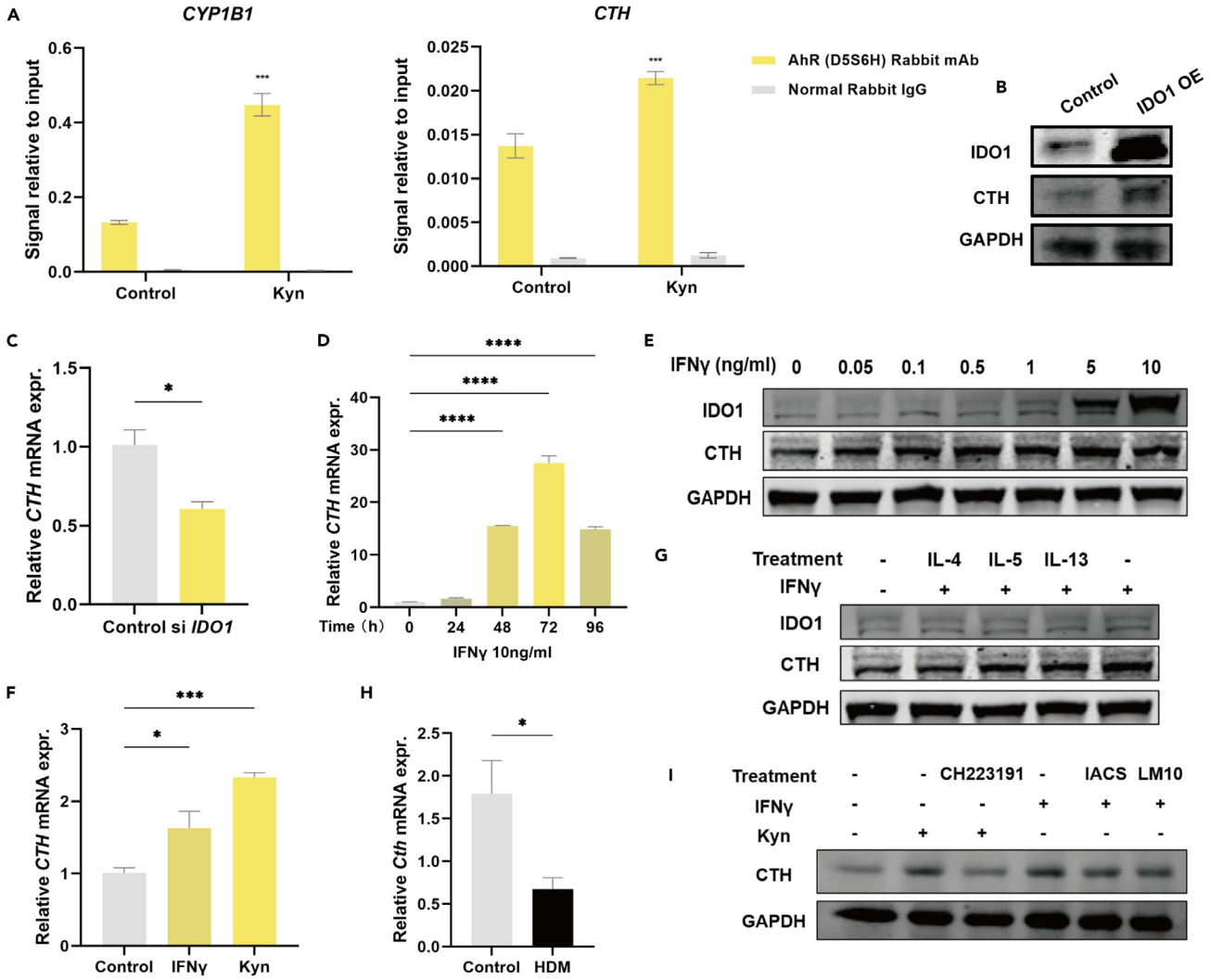

Figure 4. Kyn induces AhR translocation to regulate the transcription of the *CTH* gene

(A) ChIP-RT-PCR of *CYP1B*1 and *CTH* with the AHRE-related primer was performed. The amount of immunoprecipitated DNA in each sample was represented as a signal relative to the total amount of input chromatin, normalized to one. Data are represented as mean ± SEM. See also Figure S5B.

(B) IDO1 and CTH protein levels in BEAS-2B (pretreated with overexpression IDO1 plasmid or control).

(C) CTH mRNA levels in BEAS-2B (pretreated with si IDO1 or control). Data are represented as mean ± SEM.

(D) Under the stimulation of high concentration of IFN-γ (10 ng/ml), the expression of CTH was detected by RT-PCR at different time points. Data are represented as mean ± SEM.

(E) The expression of CTH and IDO1 were detected by western Blot with the stimulation of different concentration of IFN-γ after 48 h.

(F) Under the stimulation of IFN-γ or Kyn, the expression of CTH was detected by RT-PCR. Data are represented as mean ± SEM.

(G) The expression of CTH and IDO1 were detected by western Blot after stimulation of 10 ng/mL IL-4, IL-5, IL-13 in the presence of 100 pg/mL IFN-γ, respectively.

(H) The mRNA levels of *Cth* in lung were detected. Data are represented as mean ± SEM.

(I) The expression of CTH was detected by western blot with the treatment of IFN-γ, Kyn, IDO/TDO inhibitors, and AhR antagonist. IACS: IDO1 & TDO2 inhibitor; LM10: TDO2 inhibitor; CH223191, AhR antagonist. Data are means ± SEM. ***$p < 0.001$. One of three repeated experiments with similar results is presented. See also Figures S5 and S6.

asthma and that CTH can be regulated by IDO1-Kyn pathway. In conclusion, overexpression of IDO1 in lung relieved inflammatory infiltration and airway remodeling in HDM-induced asthma, and IDO1-Kyn-CTH pathway could be the potential mechanism.

Inhibition of CTH aggravated allergic asthma

To be clear about the specific role of CTH and hydrogen sulfide in allergic asthma, the inhibitory effect of hydrogen sulfide on airway contraction was demonstrated by shaping human primary bronchial smooth muscle cells (HBSMC) with collagen discs, finding that the centripetal

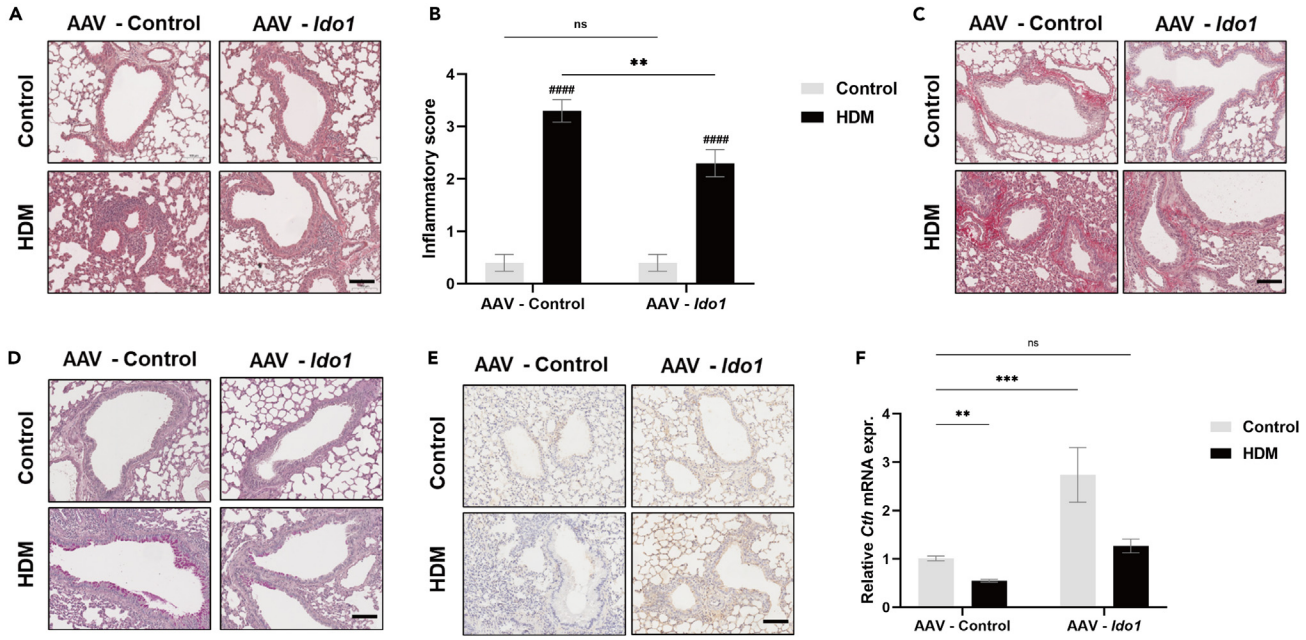

Figure 5. IDO1 overexpression relieved HDM-induced allergic asthma

(A) Representative pathological images of lung tissues by HE staining are shown.

(B) Airway and vascular inflammations were assessed. # on the column was the comparison between the control and asthma group, and * on the line was the comparison of the AAV-control and AAV-*Ido1* group. Data are represented as mean ± SEM.

(C) Subepithelial fibrosis by Sirius Red staining is shown.

(D) Mucus secretion by PAS staining is shown.

(E) The expression of CTH was detected by IHC.

(F) The mRNA level of *CTH* in lung was measured by RT-PCR. Data are represented as mean ± SEM. ####$p < 0.0001$, **$p < 0.01$, ***$p < 0.001$, ns, not significant. One of three repeated experiments with similar results is presented. The animal experiments included 6–7 BALB/c mice in each group. Scale bar, 100 μm. See also Figure S7.

contraction of the disc occurred with the treatment of histamine (Figure S8A). GYY4137, which sustained the concentration of hydrogen sulfide, slightly relieved the contraction intensity of the HBSMC collagen disc, while the application of the CTH inhibitor, PAG, resulted in increased contraction (Figures 6A–6C).

In vivo, when GYY4137 and PAG were administered in mice with HDM-induced allergic asthma, it was found that inhibition of CTH resulted in increased inflammatory infiltration, proliferation of airway epithelial goblet cells, and subepithelial fibrosis, while exogenous hydrogen sulfide supplementation relieved the exacerbation (Figures 6D, 6E, S8B and S8C). Therefore, in HDM-induced allergic asthma, CTH inhibition aggravated airway hyperresponsiveness, inflammatory cell infiltration, and airway remodeling.

DISCUSSION

Allergic asthma reflects the interaction between inflammatory mediators, immune cells, and respiratory epithelial cells. The basic mechanisms of asthma have been studied, but many questions remain. New questions on the pathogenesis of asthma continue to surface.

This study explored tryptophan metabolism in epithelial cells under T2 immune conditions *in vivo* and *in vitro* and their roles on airway remodeling. Both the increase of T2 cytokines and the decrease of T1 cytokines inhibit the expression of IDO1, resulting in a decrease in intracellular concentration of kynurenine and the inhibition of AhR activation, which is essential to maintain its transcriptional regulation of CTH. Animal experiments confirmed the relieving effect of continuous expression of IDO1 in lung tissue on airway remodeling in allergic asthma and the aggravating effect of inhibition of CTH. Finally, we also found evidence from clinical data that the ratio of serum Kyn/Trp in patients with allergic asthma was consistent with that of T1/2 cytokines, and the expression of IDO1 and CTH in airway epithelial cells were decreased.

In our study, serum Trp, but not Kyn, differed significantly between allergic asthma and healthy subjects. Trp, as a raw material, comes from the blood system, and the concentration in cells depends on the local environment of the body. The source of Kyn in serum is mainly from the KP in liver, mediated by TDO.[19] Since Kyn is an intracellular metabolite, its concentration in serum is difficult to be influenced. Therefore, detecting and targeting intervention of local tryptophan metabolism in lung is critical. A study found that inhaled corticosteroids can increase the concentration of Kyn in the sputum of patients with asthma.[20] A prospective study of the correlation between systemic tryptophan metabolism and the severity of rhinovirus-induced asthma also confirmed differences in local and systemic tryptophan catabolism.[21]

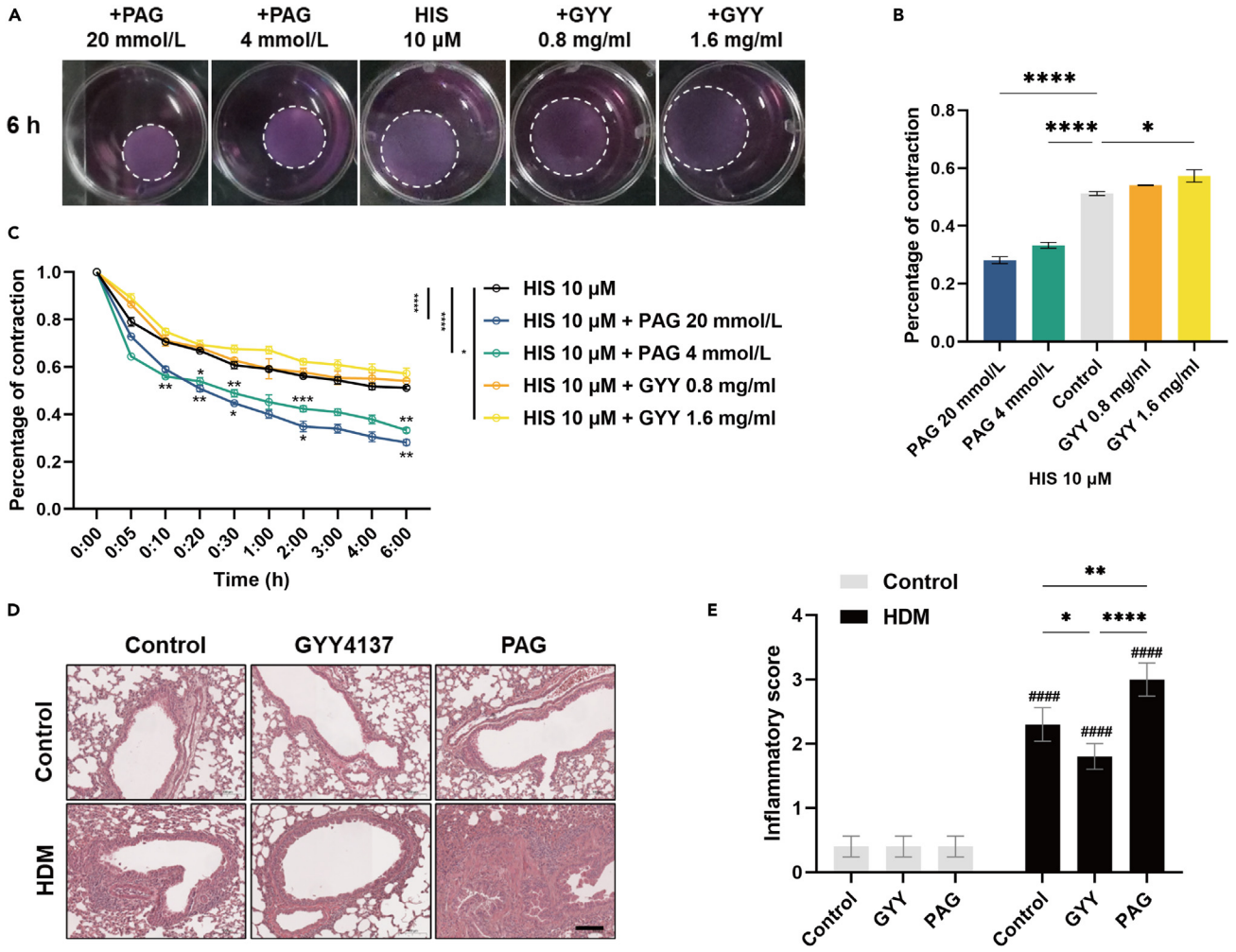

Figure 6. Inhibition of CTH aggravated allergic asthma

(A–C) The typical images (A) and percentage (B and C) of the contraction of HBSMC collagen discs in the culture medium of a 6-well plate after 6 h stimulation with PAG (20 mmol/L, 4 mmol/L) or GYY4137 (0.8 mg/mL, 1.6 mg/mL) in the presence of histamine. The circle of the white dotted line shows the range of every disc. Data are represented as mean ± SEM. See also Figure S7.

(D) Representative HE images of HDM-induced asthma lung tissues treated with GYY4137 or PAG. Scale bar, 100 μm.

(E) The airway and vascular inflammation scores were shown. Data are represented as mean ± SEM. HIS, histamine; PAG, DL-Propargylglycine, 2-Amino-4-pentanoic acid, cystathionine γ-lyase inhibitor; GYY, GYY4137. *$p < 0.05$, **$p < 0.01$, ***$p < 0.001$, ****$p < 0.0001$. One of three repeated experiments with similar results is presented. See also Figure S8.

Furthermore, we believed that the ability and effect of local tryptophan metabolism on Kyn were underestimated. IFN-γ can quickly induce IDO1 in immune cells, epithelial cells, fibroblasts, and other non-immune cells. However, it has been unanimously recognized that IDO1 inhibits tumor immunosuppression by depleting the tryptophan of immune cells by consuming high tryptophan-consuming and tryptophan-dependent cells.[5,22] Some studies have suggested that the regulation of IDO1 in T cells, macrophages, and dendritic cells plays a vital role in asthma and allergy.[23,24] A previous study has shown that the IDO activity expressed by resident lung cells rather than the IDO activity expressed by pulmonary dendritic cells inhibits pulmonary inflammation and airway hyperresponsiveness.[25] Considering the previous understanding, we focused our study on regulating airway epithelial cells by IDO1.

Additionally, hydrogen sulfide has an essential effect on inflammatory infiltration, airway hyperreactivity, and airway remodeling of asthma.[13,26,27] Nevertheless, its regulatory procedures have seldom been studied. This study reported that Kyn stimulates the expression of CTH by AhR. Additionally, we further validate the crucial role of CTH in the airway protection in allergic asthma and provide evidence for the use of H_2S-generating molecules in clinical treatment for asthma to prevent inflammatory infiltration and airway remodeling.

Therefore, ratio of kynurenine/tryptophan in serum or lower respiratory tract secretions or exhaled condensate in combination with the concentration of hydrogen sulfide is recommended pathological biomarkers of allergic asthma.

Notably, among the genes directly controlled by Kyn-AhR in epithelial cells, except for CTH, other genes still need to be investigated further. First, MUC5AC has already validated the regulation impact of AhR with other ligands on it.[28,29] However, whether the MUC5AC regulation by IDO1 can be masked by the strong induction of T2 cytokines, especially IL-13 is questionable.[30] Second, IL-24 is confirmed as a target cytokine of environmental AhR agonist exposure in the lung.[31] A recent report clarified the contribution of IL-24 to neutrophilic asthma.[32] Additionally, the balance and transformation between Th17 and Treg were correlated with AhR, and the regulation of IL17REL may be worth further discussion.

The phase III clinical trials IDO1 inhibitors as tumor immunosuppressants have failed,[5] suggesting the complexity of the physiological role of tryptophan metabolism. Our findings accurately represented the local metabolic regulation of patients with tryptophan in the lung of allergic asthma. They provided preliminary evidence for the therapeutic effect of increasing tryptophan metabolism and endogenous hydrogen sulfide generation in allergic asthma. Research in this area is expected to promote pharmaceutical development, clinical trials, and the development of new treatment modalities for allergic asthma.

In conclusion, in allergic asthma, tryptophan metabolism and IDO1-Kyn-CTH pathway is hampered by T2 inflammation, which could be a potential target for treatment. Further study still needs to clarify the specific mechanism in asthma and tryptophan metabolism.

Limitations of the study

However, this article still has aspects that need to be further studied. First, significant differences exist in the pulmonary immune microenvironment between patients with different phenotypes of asthma. The level, regulatory patterns, specific roles, and mechanism of tryptophan metabolism in lung, in different phenotypes asthma need further study. Additionally, the sample size of the clinical data are small, which may limit the reliability of the results.

STAR★METHODS

Detailed methods are provided in the online version of this paper and include the following:

- KEY RESOURCES TABLE
- RESOURCE AVAILABILITY
  - Lead contact
  - Materials availability
  - Data and code availability
- EXPERIMENTAL MODEL AND STUDY PARTICIPANT DETAILS
  - Clinical samples
  - Animal studies
  - Cell lines and cell culture
  - Ethical approval
- METHOD DETAILS
  - Cytokine analysis of serum by using multiplex bead-based immunoassay
  - RT-PCR
  - Western blotting
  - Nuclear-cytoplasmic separation experiment
  - Cell fluorescence staining
  - LC-MS/MS quantification of tryptophan metabolites
  - CUT&Tag
  - ChIP-RT-PCR validation
  - Collagen disc contraction of airway smooth muscle cells
  - Histopathology
  - Immunohistochemical staining
- QUANTIFICATION AND STATISTICAL ANALYSIS

SUPPLEMENTAL INFORMATION

Supplemental information can be found online at https://doi.org/10.1016/j.isci.2024.109923.

ACKNOWLEDGMENTS

This study was funded by National Natural Science Foundation of China (82070036), Science and Technology Commission of Shanghai Municipality (20SG38), and Shanghai Municipal Health Bureau (20XD1423300). We thank Department of Laboratory Diagnosis of Third Affiliated Hospital of Naval Medical University (Second Military Medical University) for healthy human serum, the Pathology Department of Shanghai Changzheng Hospital for lung tissues, Dong Xin Research Group of Shanghai University for mass spectrometry testing, Applied Protein Technology for MRM-based metabonomic testing, and Shanghai Jiayin for CUT&TAG testing. The authors also thank Shanghai Municipal Hospital Respiratory and Critical Care Medicine Specialist Alliance.

AUTHOR CONTRIBUTIONS

H.T., W.C., and C.B. conceived the project, designed and instructed the study, and reviewed and edited the manuscript; Y.M. and C.Z. carried out most of the experiments and prepared the original draft; S.B., K.W., and W.W. participated in clinical follow-up and blood collections; N.L. completed the part of LC-MS/MS experiments. All authors read and approved the paper.

DECLARATION OF INTERESTS

The authors declare no competing interests.

Received: December 4, 2023
Revised: March 16, 2024
Accepted: May 3, 2024
Published: May 6, 2024

REFERENCES

1. Huang, K., Yang, T., Xu, J., Yang, L., Zhao, J., Zhang, X., Bai, C., Kang, J., Ran, P., Shen, H., et al. (2019). Prevalence, risk factors, and management of asthma in China: a national cross-sectional study. Lancet (London, England) *394*, 407–418. https://doi.org/10.1016/s0140-6736(19)31147-x.
2. Kaur, R., and Chupp, G. (2019). Phenotypes and endotypes of adult asthma: Moving toward precision medicine. J. Allergy Clin. Immunol. *144*, 1–12. https://doi.org/10.1016/j.jaci.2019.05.031.
3. Akar-Ghibril, N., Casale, T., Custovic, A., and Phipatanakul, W. (2020). Allergic Endotypes and Phenotypes of Asthma. J. Allergy Clin. Immunol. Pract. *8*, 429–440. https://doi.org/10.1016/j.jaip.2019.11.008.
4. Cervenka, I., Agudelo, L.Z., and Ruas, J.L. (2017). Kynurenines: Tryptophan's metabolites in exercise, inflammation, and mental health. Science *357*, eaaf9794. https://doi.org/10.1126/science.aaf9794.
5. Platten, M., Nollen, E.A.A., Röhrig, U.F., Fallarino, F., and Opitz, C.A. (2019). Tryptophan metabolism as a common therapeutic target in cancer, neurodegeneration and beyond. Nat. Rev. Drug Discov. *18*, 379–401. https://doi.org/10.1038/s41573-019-0016-5.
6. Unuvar, S., Erge, D., Kilicarslan, B., Gozukara Bag, H.G., Catal, F., Girgin, G., and Baydar, T. (2019). Neopterin Levels and Indoleamine 2,3-Dioxygenase Activity as Biomarkers of Immune System Activation and Childhood Allergic Diseases. Ann. Lab. Med. *39*, 284–290. https://doi.org/10.3343/alm.2019.39.3.284.
7. Zhai, L., Bell, A., Ladomersky, E., Lauing, K.L., Bollu, L., Sosman, J.A., Zhang, B., Wu, J.D., Miller, S.D., Meeks, J.J., et al. (2020). Immunosuppressive IDO in Cancer: Mechanisms of Action, Animal Models, and Targeting Strategies. Front. Immunol. *11*, 1185. https://doi.org/10.3389/fimmu.2020.01185.
8. Chilosi, M., Doglioni, C., Ravaglia, C., Martignoni, G., Salvagno, G.L., Pizzolo, G., Bronte, V., and Poletti, V. (2022). Unbalanced IDO1/IDO2 Endothelial Expression and Skewed Keynurenine Pathway in the Pathogenesis of COVID-19 and Post-COVID-19 Pneumonia. Biomedicines *10*, 1332. https://doi.org/10.3390/biomedicines10061332.
9. Stockinger, B., Shah, K., and Wincent, E. (2021). AHR in the intestinal microenvironment: safeguarding barrier function. Nat. Rev. Gastroenterol. Hepatol. *18*, 559–570. https://doi.org/10.1038/s41575-021-00430-8.
10. Cheong, J.E., and Sun, L. (2018). Targeting the IDO1/TDO2-KYN-AhR Pathway for Cancer Immunotherapy - Challenges and Opportunities. Trends Pharmacol. Sci. *39*, 307–325. https://doi.org/10.1016/j.tips.2017.11.007.
11. Cirino, G., Szabo, C., and Papapetropoulos, A. (2023). Physiological roles of hydrogen sulfide in mammalian cells, tissues, and organs. Physiol. Rev. *103*, 31–276. https://doi.org/10.1152/physrev.00028.2021.
12. Ivanciuc, T., Sbrana, E., Casola, A., and Garofalo, R.P. (2019). Cystathionine gamma-lyase deficiency enhances airway reactivity and viral-induced disease in mice exposed to side-stream tobacco smoke. Pediatr. Res. *86*, 39–46. https://doi.org/10.1038/s41390-019-0396-6.
13. Wang, P., Wu, L., Ju, Y., Fu, M., Shuang, T., Qian, Z., and Wang, R. (2017). Age-Dependent Allergic Asthma Development and Cystathionine Gamma-Lyase Deficiency. Antioxid. Redox Signal. *27*, 931–944. https://doi.org/10.1089/ars.2016.6875.
14. Pacitti, D., Scotton, C.J., Kumar, V., Khan, H., Wark, P.A.B., Torregrossa, R., Hansbro, P.M., and Whiteman, M. (2021). Gasping for Sulfide: A Critical Appraisal of Hydrogen Sulfide in Lung Disease and Accelerated Aging. Antioxid. Redox Signal. *35*, 551–579. https://doi.org/10.1089/ars.2021.0039.
15. Liu, Y., Liang, X., Dong, W., Fang, Y., Lv, J., Zhang, T., Fiskesund, R., Xie, J., Liu, J., Yin, X., et al. (2018). Tumor-Repopulating Cells Induce PD-1 Expression in CD8(+) T Cells by Transferring Kynurenine and AhR Activation. Cancer Cell *33*, 480–494.e7. https://doi.org/10.1016/j.ccell.2018.02.005.
16. Sadik, A., Somarribas Patterson, L.F., Öztürk, S., Mohapatra, S.R., Panitz, V., Secker, P.F., Pfänder, P., Loth, S., Salem, H., Prentzell, M.T., et al. (2020). IL4I1 Is a Metabolic Immune Checkpoint that Activates the AHR and Promotes Tumor Progression. Cell *182*, 1252–1270.e1234. https://doi.org/10.1016/j.cell.2020.07.038.
17. Zhang, X., Gan, M., Li, J., Li, H., Su, M., Tan, D., Wang, S., Jia, M., Zhang, L., and Chen, G. (2020). Endogenous Indole Pyruvate Pathway for Tryptophan Metabolism Mediated by IL4I1. J. Agric. Food Chem. *68*, 10678–10684. https://doi.org/10.1021/acs.jafc.0c03735.
18. Davoodi, P., Mahesh, P.A., Holla, A.D., Vijayakumar, G.S., Jayaraj, B.S., Chandrashekara, S., and Ramachandra, N.B. (2012). Serum levels of interleukin-13 and interferon-gamma from adult patients with asthma in Mysore. Cytokine *60*, 431–437. https://doi.org/10.1016/j.cyto.2012.05.012.
19. Modoux, M., Rolhion, N., Mani, S., and Sokol, H. (2021). Tryptophan Metabolism as a Pharmacological Target. Trends Pharmacol. Sci. *42*, 60–73. https://doi.org/10.1016/j.tips.2020.11.006.
20. Maneechotesuwan, K., Supawita, S., Kasetsinsombat, K., Wongkajornsilp, A., and Barnes, P.J. (2008). Sputum indoleamine-2, 3-dioxygenase activity is increased in asthmatic airways by using inhaled corticosteroids. J. Allergy Clin. Immunol. *121*, 43–50. https://doi.org/10.1016/j.jaci.2007.10.011.
21. van der Sluijs, K.F., van de Pol, M.A., Kulik, W., Dijkhuis, A., Smids, B.S., van Eijk, H.W., Karlas, J.A., Molenkamp, R., Wolthers, K.C., Johnston, S.L., et al. (2013). Systemic tryptophan and kynurenine catabolite levels relate to severity of rhinovirus-induced asthma exacerbation: a prospective study with a parallel-group design. Thorax *68*, 1122–1130. https://doi.org/10.1136/thoraxjnl-2013-203728.
22. Bartok, O., Pataskar, A., Nagel, R., Laos, M., Goldfarb, E., Hayoun, D., Levy, R., Körner, P.R., Kreuger, I.Z.M., Champagne, J., et al. (2021). Anti-tumour immunity induces aberrant peptide presentation in melanoma. Nature *590*, 332–337. https://doi.org/10.1038/s41586-020-03054-1.
23. Hu, Q., Jin, L., Zeng, J., Wang, J., Zhong, S., Fan, W., and Liao, W. (2020). Tryptophan metabolite-regulated Treg responses contribute to attenuation of airway inflammation during specific immunotherapy in a mouse asthma model. Hum. Vaccin. Immunother. *16*, 1891–1899. https://doi.org/10.1080/21645515.2019.1698900.
24. Hayashi, T., Mo, J.H., Gong, X., Rossetto, C., Jang, A., Beck, L., Elliott, G.I., Kufareva, I., Abagyan, R., Broide, D.H., et al. (2007). 3-Hydroxyanthranilic acid inhibits PDK1 activation and suppresses experimental asthma by inducing T cell apoptosis. Proc. Natl. Acad. Sci. USA *104*, 18619–18624. https://doi.org/10.1073/pnas.0709261104.
25. Hayashi, T., Beck, L., Rossetto, C., Gong, X., Takikawa, O., Takabayashi, K., Broide, D.H., Carson, D.A., and Raz, E. (2004). Inhibition of experimental asthma by indoleamine 2,3-dioxygenase. J. Clin. Invest. *114*, 270–279. https://doi.org/10.1172/jci21275.

26. Zhang, J., Wang, X., Chen, Y., and Yao, W. (2014). Correlation between levels of exhaled hydrogen sulfide and airway inflammatory phenotype in patients with chronic persistent asthma. Respirology *19*, 1165–1169. https://doi.org/10.1111/resp.12372.
27. Bazhanov, N., Ansar, M., Ivanciuc, T., Garofalo, R.P., and Casola, A. (2017). Hydrogen Sulfide: A Novel Player in Airway Development, Pathophysiology of Respiratory Diseases, and Antiviral Defenses. Am. J. Respir. Cell Mol. Biol. *57*, 403–410. https://doi.org/10.1165/rcmb.2017-0114TR.
28. Hu, X., Shen, Y., Zhao, Y., Wang, J., Zhang, X., Tu, W., Kaufman, W., Feng, J., and Gao, P. (2021). Epithelial Aryl Hydrocarbon Receptor Protects From Mucus Production by Inhibiting ROS-Triggered NLRP3 Inflammasome in Asthma. Front. Immunol. *12*, 767508. https://doi.org/10.3389/fimmu.2021.767508.
29. Sun, Y., Shi, Z., Lin, Y., Zhang, M., Liu, J., Zhu, L., Chen, Q., Bi, J., Li, S., Ni, Z., and Wang, X. (2021). Benzo(a)pyrene induces MUC5AC expression through the AhR/mitochondrial ROS/ERK pathway in airway epithelial cells. Ecotoxicol. Environ. Saf. *210*, 111857. https://doi.org/10.1016/j.ecoenv.2020.111857.
30. Siddiqui, S., Johansson, K., Joo, A., Bonser, L.R., Koh, K.D., Le Tonqueze, O., Bolourchi, S., Bautista, R.A., Zlock, L., Roth, T.L., et al. (2021). Epithelial miR-141 regulates IL-13-induced airway mucus production. JCI insight *6*, e139019. https://doi.org/10.1172/jci.insight.139019.
31. Luo, Y.H., Kuo, Y.C., Tsai, M.H., Ho, C.C., Tsai, H.T., Hsu, C.Y., Chen, Y.C., and Lin, P. (2017). Interleukin-24 as a target cytokine of environmental aryl hydrocarbon receptor agonist exposure in the lung. Toxicol. Appl. Pharmacol. *324*, 1–11. https://doi.org/10.1016/j.taap.2017.03.019.
32. Feng, K.N., Meng, P., Zhang, M., Zou, X.L., Li, S., Huang, C.Q., Lai, K.F., Li, H.T., and Zhang, T.T. (2022). IL-24 Contributes to Neutrophilic Asthma in an IL-17A-Dependent Manner and Is Suppressed by IL-37. Allergy Asthma Immunol. Res. *14*, 505–527. https://doi.org/10.4168/aair.2022.14.5.505.
33. Kaya-Okur, H.S., Wu, S.J., Codomo, C.A., Pledger, E.S., Bryson, T.D., Henikoff, J.G., Ahmad, K., and Henikoff, S. (2019). CUT&Tag for efficient epigenomic profiling of small samples and single cells. Nat. Commun. *10*, 1930. https://doi.org/10.1038/s41467-019-09982-5.
34. Sakota, Y., Ozawa, Y., Yamashita, H., Tanaka, H., and Inagaki, N. (2014). Collagen gel contraction assay using human bronchial smooth muscle cells and its application for evaluation of inhibitory effect of formoterol. Biol. Pharm. Bull. *37*, 1014–1020. https://doi.org/10.1248/bpb.b13-00996.
35. Zhang, G., Wang, P., Yang, G., Cao, Q., and Wang, R. (2013). The inhibitory role of hydrogen sulfide in airway hyperresponsiveness and inflammation in a mouse model of asthma. Am. J. Pathol. *182*, 1188–1195. https://doi.org/10.1016/j.ajpath.2012.12.008.

STAR★METHODS

KEY RESOURCES TABLE

REAGENT or RESOURCE	SOURCE	IDENTIFIER
Antibodies		
Rabbit polyclonal anti- IDO1	Cell Signaling Technology	Cat#3879S; RRID: AB_2255011
Mouse monoclonal anti-Tubulin (clone DM1A)	Sigma-Aldrich	Cat#T9026; RRID: AB_477593
Rabbit polyclonal anti- IDO1	Proteintech	Cat#13268-1-AP; RRID: AB_2123444
Rabbit polyclonal anti- Lamin B1	Abcam	Cat#ab16048; RRID: AB_443298
Rabbit Polyclonal anti-CTH	Absin	Cat# abs128251; RRID: AB_3094672
Mouse monoclonal anti-β-Actin	Cell Signaling Technology	Cat#3700; RRID: AB_2242334
Rabbit monoclonal anti -α-SMA	Cell Signaling Technology	Cat# 19245; RRID: AB_2734735
Rabbit monoclonal anti- AhR	Cell Signaling Technology	Cat#83200; RRID: AB_2800011
Rabbit monoclonal anti -GAPDH	Cell Signaling Technology	Cat#2118; RRID: AB_561053
Bacterial and virus strains		
pAAV-CMV-Ido1-3xFLAG-EF1-GdGreen-WPRE	Shanghai OBiO	N/A
pAAV-CMV-EF1-GdGreen-WPRE	Shanghai OBiO	N/A
Chemicals, peptides, and recombinant proteins		
Recombinant Human IL-4 Protein	Absin	abs04698;
Recombinant Human IL-5 Protein	Absin	abs04445
Recombinant Human IL-13 Protein	Absin	abs00816
Recombinant Human IFN-γ Protein	Absin	abs04123
L-Tryptophan	Absin	abs47000171
L-Kynurenine	Absin	abs821876
IACS-8968	MCE	HY-112164
LM10	MCE	HY-33298
CH223191	MCE	HY-12684
HDM	Stallergenes	XPB81D3A2.5
Histamine	Absin	abs47047849
GYY4137	MCE	HY-107632
PAG	Sigma	P7888
Critical commercial assays		
Human Cytokine/Chemokine Magnetic Bead Panel	Bio-Rad	#HCYTA-60K-PX48
Pierce Agarose ChIP Kit	Thermo	26156
Deposited data		
Raw data	This paper	SRA: PRJNA1087459
Experimental models: Cell lines		
Human: BEAS-2B cells	ATCC	CRL-3588
Human: HBSMC cells	ATCC	PCS-130-011
Experimental models: Organisms/strains		
BALB/c	SPF Biotechnology Co., Ltd	N/A
Oligonucleotides		
Primers for RT-PCR, see Table S5	This paper	N/A
Recombinant DNA		
Ubi-MCS-3FLAG-CBh-gcGFP-IRES-puromycin	Genechem	N/A

(*Continued on next page*)

Continued

REAGENT or RESOURCE	SOURCE	IDENTIFIER
Ubi-IDO1-3FLAG-CBh-gcGFP-IRES-puromycin	Genechem	N/A
Plasmid-shRNA-JAK1	Genechem	N/A
Plasmid- shRNA-Control	Genechem	N/A
Plasmid-siRNA-IDO1	Shanghai OBiO	N/A
Plasmid- siRNA-Control	Shanghai OBiO	N/A
Software and algorithms		
GraphPad Prism V9.0.0	GraphPad	https://www.graphpad.com/

RESOURCE AVAILABILITY

Lead contact

Further information and requests for resources should be directed to and will be fulfilled by the lead contact, Hao Tang (tanghao_0921@126.com).

Materials availability

This study did not generate new unique reagents.

Data and code availability

- All data reported in this paper will be shared by the lead contact upon request.
- Raw data of CUT&Tag has been uploaded in SRA database: PRJNA1087459.
- This paper does not report original code.
- Any additional information required to reanalyze the data reported in this paper is available from the lead contact upon request.

EXPERIMENTAL MODEL AND STUDY PARTICIPANT DETAILS

Clinical samples

The lung tissues were collected in the pathology department of Shanghai Changzheng Hospital from 2018 to 2022. Most of them were para-cancer tissue, surgical margin and bronchial stump retained after surgery of lung cancer, and a few of them were inflammatory masses proved after resection of pulmonary nodules. All participants are Chinese with age ranging from 20 to 80. Participants with asthma have the history of asthma ranging from 3 to 30 years. At the same time, patients without asthma and related inflammatory disease were selected for healthy control. More details are in Table S1.

The serum from asthma patients and health controls were the remaining samples after clinical testing from Department of Respiratory and Critical Care Medicine of Shanghai Changzheng Hospital and Department of Laboratory Diagnosis of Third Affiliated Hospital of Naval Medical University (Second Military Medical University), respectively. The health controls are people for health examination without asthma history. All participants are Chinese with age ranging from 50 to 75. More details are in Table S2.

Animal studies

Female BALB/c mice (SPF Biotechnology Co., Ltd, Beijing, China) between 7 and 8 weeks (20–23 g) were used. All mice were maintained under pathogen-free conditions. The health of the mice was monitored every other day.

To study the effect of the administration of exogenous hydrogen sulfide or CTH inhibitor (PAG) on the severity of HDM-induced asthma, intraperitoneal injections of PAG (200 μL, 5 mg/mL, 50 mg/kg/day) or GYY4137 (200 μL, 0.5 mg/mL, 5 mg/kg/day) were administered every day during the establishment of the model. The control group received 200 μL of PBS. Nasal drops of HDM or PBS were applied 30 min after treatment with PAG and GYY41337 to ensure the effect of PAG and GYY41337.

Pneumophilic adeno-associated virus (serotype AAV2/LUNG) carrying Ido1 (pAAV-CMV-Ido1-3xFLAG-EF1-GdGreen-WPRE) and control adeno-associated virus (pAAV-CMV-EF1-GdGreen-WPRE) were constructed by Shanghai OBiO Technology. Intratracheal instillation of AAV ($1.5 * 10^{11}$ v.g./mice) was 24 h before day 0 of the asthma model. Two mice were killed on day 21 to determine the infection of AAV and the overexpression of Ido1 in the lungs.

Cell lines and cell culture

Human lung airway epithelial cell line Beass-2B (Shanghai Zhong Qiao Xin Zhou Biotechnology Co.,Ltd.) were cultured in Dulbecco's Modified Eagle Medium (DMEM, Gibco), high glucose (4500 mg/L) media with 10% fetal bovine serum (FBS) and 1% penicillin/streptomycin. For metabolite-related experiments, cells were washed once with phosphate-buffered saline (PBS) and then incubated in Ham's F-10 medium

(Gibco), which is tryptophan-deficient with only 3 μM tryptophan, and extra tryptophan was added to control tryptophan concentration while the indicated stimulus was added for a specific time. Cells were incubated in basal DMEM medium with 10% FBS, indicating stimulus for other experiments.

Primary human bronchial smooth muscle cells (HBSMC) (Shanghai Zhong Qiao Xin Zhou Biotechnology Co.,Ltd.) were cultured in smooth muscle cell medium (SMCM, Sciencell). To conduct the experiments, cells were washed with PBS once and then incubated with DMEM medium and the indicated stimuli.

Ethical approval

The part of study related to both the clinical samples and animal models was approved by the Medical Ethics Committee of Shanghai Changzheng Hospital. Informed consents were achieved.

METHOD DETAILS

Cytokine analysis of serum by using multiplex bead-based immunoassay

Human cytokines in the serum were measured by Bio-plex Pro TM Human Cytokine Screening 48 plex Bio-PlexTM 200 System (#12007283, Bio-Rad, US) and Human Cytokine/Chemokine Magnetic Bead Panel (#HCYTA-60K-PX48). The experiments were performed following the manufacturers' instructions. The samples were diluted 4-fold (1:4) by adding 1 volume of sample to 3 volumes of sample diluent. Fifty microliters of each sample were used to assay.

RT-PCR

Total RNA from BEAS-2B cells or mouse lung was isolated by Trizol reagent (life, 15596018). Lung tissues need to be ground to allow for adequate RNA extraction. Reverse transcription was performed using the One-Step RT-PCR kit (Vazyme). Complementary DNA was generated by SuperScript III (Vazyme), and SYBR Green PCR master mix (Vazyme) was used for RT-PCR. The amount of mRNA was normalized to GAPDH.

Western blotting

The lysis buffer of mouse lung and human BEAS-2B cells were RIPA and IP lysis buffer (Beyotime), respectively. Supplemented with Protease Inhibitor Cocktail (Sigma-Aldrich). Proteins were separated by sodium dodecyl sulfate polyacrylamide gel electrophoresis (SDS-PAGE) and transferred to NC membranes, and the blots were blocked with 5% bovine serum albumin in TBS buffer. The blots were sequentially treated with primary and secondary antibodies. The blots were imaged by Odyssey CLx imaging system.

Nuclear-cytoplasmic separation experiment

To detect AhR subcellular location, cytoplasm and nuclear extracts were prepared with NE-PER Nuclear and Cytoplasmic Extraction Reagent (Pierce, Thermo Scientific, USA) following the manufacturer's instructions. Separated cytoplasmic and nuclear were Quantified and tested by Western blotting using GAPDH for cytoplasmic protein and LaminB for nuclear protein.

Cell fluorescence staining

Cells were fixed with 4% paraformaldehyde, permeabilized with 0.5% Triton X-100, and blocked with 2% BSA for 1 h at RT. Samples were incubated with anti-AhR antibody (1:100, Abcam, ab84833) for 1 h at room temperature or overnight at 4°C. Alexa fluor secondary antibody (1:500) was used. DAPI (1 μg/mL) was used to visualize the nucleus. Confocal microscope was used for images.

LC-MS/MS quantification of tryptophan metabolites

Cell samples were homogenate using Biospec MiniBeadbeater24. The supernatant was injected for HPLC-MS/MS analysis. The separation was performed on a UPLC system (Agilent 1290 Infinity UHPLC) on a C-18 column (Waters, CSH C18 1.7 μm, 2.1 × 100 mm column) by gradient elution. The MRM method was used for mass spectrometry quantitative data acquisition. The 23 metabolites analyzed are listed in Table S4. MultiQuant or Analyst was used for quantitative data processing. The integration was further checked manually.

CUT&Tag

CUT&Tag assay was performed as previously described with modifications.[33] A total of 100000 cells were used for each group, and a 1:50 dilution of AhR (D5S6H) Rabbit antibody (CST#83200) or normal rabbit IgG (Millipore cat no. 12–370) control antibody was used for incubation. DNA was purified and amplify libraries. Sequencing was performed in the Illumina Novaseq 6000 using a 150 bpa paired end following the manufacturer's instructions.

After quality control and reads mapping to the reference genome, the bam file generated by the unique mapped reads as an input file, using macs2 software for callpeak with cutoff qvalue <0.05. Then, The HOMER's findMotifsGenome.pl tool was used for Motif analysis. Peaks were annotated by using homer's annotatePeaks.pl. Count the results of the annotations and plot the distribution results using R.

ChIP-RT-PCR validation

Chromatin immunoprecipitation (ChIP) assays were performed using Pierce Agarose ChIP Kit (Thermo, 26156) following the manufacturer's instructions with cross-linked chromatin from BEAS-2B cells treated with Kyn or not using AhR(D5S6H) Rabbit mAb (1:50, CST, 83200) and normal Rabbit IgG (CST, 2729). The enriched DNA was quantified by real-time PCR using human *CYP1B1* promoter primers. The amount of immunoprecipitated DNA in each sample was represented as a signal relative to the total amount of input chromatin, equivalent to one. Sequences for RT-PCR primers of *CYP1B1* promoter included AhRE: forward (5′→3′): CCCTAAAAGTAGCCGCTCCC; reverse (5′→3′): ATGACTGGAGCCGACTTTCC. Primer of *CTH* promoter included AhRE: forward (5′→3′): AAATCCACCCCAACAATCGC; reverse (5′→3′): GTGGCAGGAAACCTTGTGAG.

Collagen disc contraction of airway smooth muscle cells

According to previous report,[34] the assay was improved as follows. Type I collagen solution (5 mg/mL), HBSMC suspension ($8*10^5$/mL), DMEM, NaOH (24 μM), GYY4137 (0.01M), PAG (0.01M) and histamine (0.01M) bacteria-free solution were prepared and stored at 4°C. The groups are as follows. Group black-control, (collagen + cell) + DMEM; Group A, (collagen + cell) + DMEM containing histamine (10 μM); Group B, (collagen + cell) containing GYY4137 (0.8 mmol/L) + DMEM containing histamine (10 μM); Group C, (collagen + cell) containing GYY4137 (1.6 mmol/L) + DMEM containing histamine (10 μM); Group D, (collagen + cell) containing PAG (4 mmol/L) + DMEM containing histamine (10 μM); Group E, (collagen + cell) containing PAG (20 mmol/L) + DMEM containing histamine (10 μM). Mix the prepared materials on ice carefully, except histamine and DMEM, according to the grouping requirements, and placed 500 μL in 24-well plates. The mixture in each well contained 1 mg/mL of collagen, 2×10^5 cells, PH neutral. Collagen coagulated after 20–30 min at RT. Then, according to the grouping, DMEM and histamine were added to the well, and the collagen discs were separated by tip to make them suspended. 24-well plate was cultured in incubator at 37°C. Take photos at 0 min, 5 min, 10 min, 20 min, 30 min, 40 min, 50 min, 60 min, 2 h, 3 h, 4 h, 5 h, 6 h (keep the distance between the camera and the plate constant). Use ImageJ to measure the area of discs, and compare with the area of the well, as a value of the percentage of contraction.

Histopathology

Pathological staining use Paraffin-embedded sections at 4 μm. The lung sections were stained with hematoxylin and eosin (H&E) to assess the inflammatory cells infiltrate, Masson's trichrome and Sirius Red to determine the collagen deposition in the lungs, and periodic acid-Schiff (PAS) to identify airway goblet cells. Peribronchial and perivascular inflammation in H&E-stained slides was assessed using a scoring standard as previously described.[35] 0 = normal; 1 = infrequent inflammatory cells; 2 = a ring of inflammatory cells 1 cell layer deep; 3 = a ring of inflammatory cells 2–4 cells deep and 4 = a ring of inflammatory cells more than 4 cells deep. Scores were done by two experienced pathologists blinded to testing. Two scores were taken and the average value noted.

Immunohistochemical staining

Briefly, the tissues were embedded with paraffin using conventional method. They were cut into 5 μm slices, and incubated with 0.3% endogenous peroxidase blocking solution for 20 min after dewaxing and hydrating. Then they were incubated at room temperature for 10 min with 3% hydrogen peroxide methanol solution, and washed with PBS for 3 times (5 min/time). Antigen retrieval was performed using citrate buffer (pH 6.0) or Tris-EDTA (pH 9.0) at 121°C for 2 min. After blocking with 5% BSA, they were incubated with a primary monoclonal antibody overnight at 4°C. Staining was visualized by Dako REAL EnVision Detection System, Peroxidase/DAB+, Rabbit/Mouse (K5007, Dako) followed by counterstaining with hematoxylin. They were then mounted with epoxy resin. Images were captured using a digital camera (DP73, Olympus) under a light microscope (BX53, Olympus).

QUANTIFICATION AND STATISTICAL ANALYSIS

Statistical analysis was performed using GraphPad Prism 9. The results were expressed as mean ± SEM if not otherwise specified. The two-tailed Student's t-test and ANOVA were used when the data were normally distributed, and the variance was homogeneous. In cases where the normal distribution was not satisfied, and the variance was homogeneous, the rank-sum test was used. The results were considered significant at $p < 0.05$.